Generation of longitudinally polarized multi-segment optical needles by tightly focusing RPBG beam*

SHI Changkun[1], SONG Yiding[2], DONG Bing[1], ZHOU Zhanqi[1], ZHANG Zengqi[1], and XU Zongwei[1]**

1. State Key Laboratory of Precision Measuring Technology & Instruments, Tianjin University, Tianjin 300072, China

2. School of Optical-Electrical and Computer Engineering, University of Shanghai for Science and Technology, Shanghai 200093, China

(Received 1 November 2022; Revised 15 January 2023)

In this paper, an effective method to garner sub-wavelength longitudinally polarized multi-segment optical needle sequence by using a specially designed hybrid filter (HF) in a high numerical aperture (*NA*) objective focusing system is proposed. The HF is coupled by a binary phase transmission function and a multi-segment modulation function, and the binary phase filter is designed by the particle swarm optimization (PSO) algorithm and acts on the radially polarized Bessel Gaussian (RPBG) beam to obtain a longitudinally polarized optical needle with long depth of focus (*DOF*, 6λ) and a sub-wavelength transverse spot size (0.430λ). The optical needle is with high uniformity of 98% and high beam quality of 96%, and the negligible sidelobe is 15%. On this basis, the multi-segment optical needle sequence with tunable spacing or number can be realized by the multi-segment modulation function. It is found that the HF makes the generation of multi-segment optical needle sequence more flexible and reliable. This research has broad application prospects in material processing, particle acceleration, particle capture and other fields.

Document code: A **Article ID:** 1673-1905(2023)07-0399-6

DOI https://doi.org/10.1007/s11801-023-2184-0

Based on the non-diffraction characteristics of Bessel Gaussian (BG) beam, the research of using BG vector light field to generate super-resolution light field in high numerical aperture (*NA*) objective lens system has been a hot topic in the research of light field modulation. In related research, by using the amplitude and phase modulation, the radially polarized Bessel Gaussian (RPBG) beam can generate an optical needle with strong longitudinally polarized composition, which has a wide range of applications in super-resolution microscopic imaging[1-3], optical micromanipulation[4,5], femtosecond laser micro-nano processing[6-8] and high-density optical data storage[9,10]. Under the condition of tight focusing, the longitudinally polarized optical needle opens up a new field of the research of light field modulation because of its special polarization composition, super resolution transverse spot size and long depth of focus (*DOF*).

Since the method of producing longitudinally polarized optical needles in a high *NA* objective by modulating RPBG beams with a binary phase filter was reported[11], more and more methods have been applied to the generation of optical needles with extremely long focusing depth and sub-diffraction transverse resolution, such as different optical systems[12-14], different vector-polarized light sources[15-17] and different binary phase filters[18,19]. In addition, many attempts have been made to generate sub-diffractive optical needles using special media or lenses. At present, optical needles have shown superior performance in applications related to stimulated emission depletion (STED)[20] and chiral materials sorting[13]. However, for the practical applications, the application efficiency of single optical needle is low, so the application of the modulation method generating the optical needle arrays can effectively improve the efficiency of the optical needle in the relevant application. YU et al[21] reported a method for generating multistage optical needles in a 4π optical system by inverting the radiation field of an electric dipole array. Multi-segment optical needles can control the number of optical needles in the array and the spacing of adjacent optical needles to realize the adjustment of focal length and spacing. At present, the *DOF* of the single optical needle obtained by different types of light sources or modulation methods is limited. The optical needle modulation method with an ultra-long *DOF* brings great pressure to the optimization algorithm, and it is difficult to ensure the uniformity of the light field intensity of the optical needle. Therefore, the generation and application of multi-segment optical

* This work has been supported by the '111' Project by the State Administration of Foreign Experts Affairs, the 2020 Mobility Programme of the Sino-German Center for Research Promotion (M-0396), the Ministry of Education of China (No.B07014), the National Natural Science Foundation of China (Nos.11974258 and 11604236), and the Key Research and Development (R&D) Projects of Shanxi Province (No.201903D121127).

** E-mail: zongweixu@tju.edu.cn

needle sequence will make up for the lack of axial focusing ability of the single optical needle. For example, LUO et al[22] garnered a three-dimensional (3D) magnetized needle array with arbitrary orientation, controllable number, and spacing in a high *NA* objective lens focusing system. The transverse size of the magnetized needle in the array is 0.36λ, and the *DOF* is 5.36λ. The number and position of the needle array can be flexibly modulated in the focusing volume. It can be seen that the research of using different optical systems or different optical modulation methods to generate 3D multi-focal optical needle arrays is gradually attracting people's attention.

In this paper, a hybrid filter (HF) coupled by a binary phase filter and a pure-phase filter is proposed to generate longitudinally polarized multi-segment optical needle sequences. Based on the vector diffraction theory, the binary phase filter transmissive function after being processed by the particle swarm optimization (PSO) algorithm is coupled with the multi-segment modulation function, and acted on an RPBG beam to garner the multi-segment optical needle sequence in a high *NA* objective lens system. Then, the multi-segment optical needle sequences with different spacings and numbers of optical needles are generated and analyzed. This method has excellent flexibility and provides a reliable technical path for the generation of 3D multi-focal needle array.

Fig.1(a) presents the principle of generating the multi-segment optical needles by focusing an RPBG beam in a high *NA* focusing system. The phase of the RPBG beam in the pupil plane is modulated by the HF. Subsequently, the multi-segment optical needle sequence can be generated in the focusing space through a high *NA* objective lens. The geometric focal spots *O* represent the origin of rectangular coordinates (x, y, z) and cylindrical coordinates (r, φ, z).

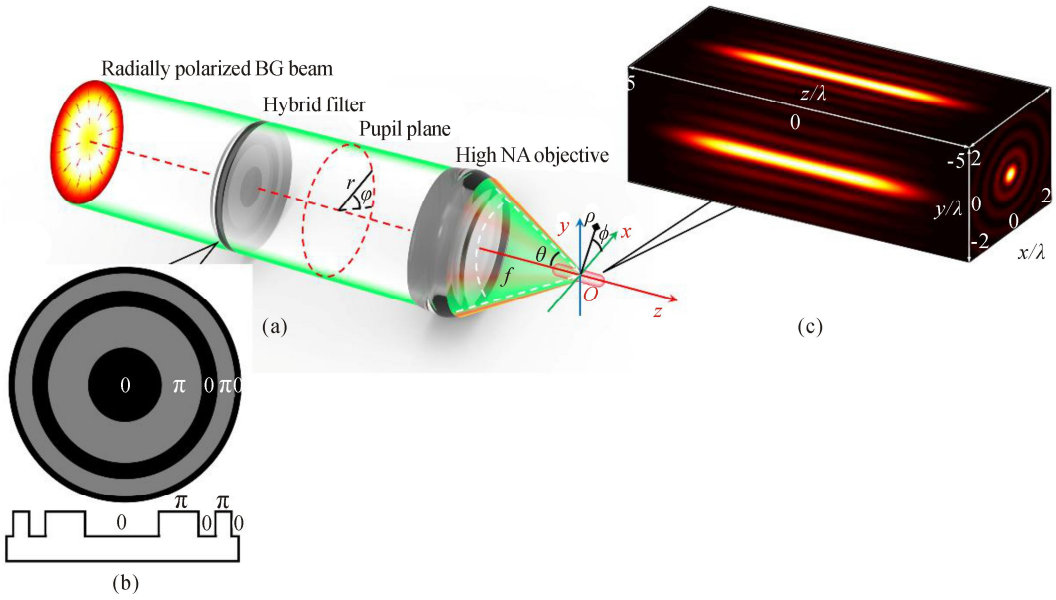

Fig.1 Principle of single optical needle generated by tightly focused RPBG beam with the modulation of the HF filter in the high *NA* objective system: (a) High *NA* objective focusing system with the HF; (b) Structure of the HF to generate the single optical needle; (c) Electric field of the optical needle in the focus space

Based on the vector diffraction theory[23], in the high *NA* objective focusing system, the electric fields of the tightly focused RPBG beam in the focus region can be expressed as

$$\boldsymbol{E}(r,z)=E_r(r,z)\boldsymbol{e}_r+E_z(r,z)\boldsymbol{e}_z, \tag{1}$$

where $\boldsymbol{e}_r$ and $\boldsymbol{e}_z$ are the unit vectors in the radial and axial directions, respectively. $E_r(r, z)$ and $E_z(r, z)$ are the amplitude distributions along the unit vectors $\boldsymbol{e}_r$ and $\boldsymbol{e}_z$ in the focusing space written as

$$E_r(r,z)=A\int_0^{\alpha}\sin(2\theta)\cos^{1/2}(\theta)l_0(\theta)\cdot M(\theta)J_1(kr\sin\theta)\mathrm{e}^{\mathrm{i}kz\cos\theta}\mathrm{d}\theta, \tag{2}$$

and

$$E_z(r,z)=2\mathrm{i}A\int_0^{\alpha}\sin^2(\theta)\cos^{1/2}(\theta)l_0(\theta)\cdot M(\theta)J_0(kr\sin\theta)\mathrm{e}^{\mathrm{i}kz\cos\theta}\mathrm{d}\theta, \tag{3}$$

where A is the amplitude constant, θ is the value of the convergence, α=arcsin(NA/n_0) is the maximum value of θ, and the refraction index of the medium is $n_0\cdot k=2\pi/\lambda$, k represents the wave number in free space, and λ is the incident laser wavelength. J_n is the Bessel function of the first kind with order n (n=0, 1). $l_0(\theta)$ is the amplitude distribution of the incident BG beam, which can be expressed as

$$l_0(\theta)=\mathrm{e}^{-(\beta_0\sin\theta/\sin\alpha)^2}\cdot J_n(2\beta_0\sin\theta/\sin\alpha). \tag{4}$$

For $l_0(\theta)$, β_0 is the truncation parameter. $M(\theta)$ is the transmission function of the HF, which can be written as Eq.(5a)[24]

$$M(\theta)=T(\theta)\cdot P(z_d), \tag{5a}$$

$$T(\theta)=\frac{1}{2}\sum_{i=1}^{N}(A_i\cos\theta\cdot\sin^3\theta)\cdot\left[\mathrm{e}^{\mathrm{i}\frac{2\pi k_i\theta}{\alpha}}+\mathrm{e}^{-\mathrm{i}\frac{2\pi k_i\theta}{\alpha}}\right], \quad (5b)$$

$$P(z_d)=\sum_{d=1}^{D}\exp(\pm\mathrm{i}k(z_d-z_0)\cos\theta), \quad (5c)$$

where $T(\theta)$ is the transmission function of the optical needle. N is the number of the belts. A_i is the amplitude coefficient, and $\cos\theta\cdot\sin^3\theta$ is the coefficient of compressibility. k_i is the phase coefficient. To generate an optical needle, the amplitude coefficient A_i and phase coefficient s_i need to be optimized with a PSO algorithm[25]. To garner a multi-segment optical needle sequence, the multi-segment modulation function $P(z_d)$ is introduced in the HF. For the multi-segent modulation function $P(z_d)$, the parameter D is integer, giving the total number of the prescribed unit optical needle of the multi-segment optical needle sequence. The range of d is (1~D), and ($-z_d+z_0$) denotes the axial displacement of the optical needle in the multi-segment optical needle sequence. The parameters z_d and z_0 represent the spatial coordinates and the origin of spatial rectangular coordinate system, respectively.

To generate the phase diagram of the multi-segment optical needle sequence, the HF is adopted to encode the spatial phase of tightly focused vector light beams. Based on the vector diffraction theory, the parameters n_0=1, NA=0.95, λ=515 nm are set in Eqs.(2) and (3), and the truncation parameter β_0 for the Gaussian beam and the BG beam is set to 1. Subsequently, the multi-segment optical needle sequences are generated with the RPBG beam.

Before generating the multi-segment light needle sequence, we first generated a single light needle in the focusing space by using HF modulated RPBG beam. The normalized electric field intensity distribution of the single light needle is shown in Fig.1(c). For the single optical needle, the amplitude coefficient A_i and phase coefficient k_i, which are processed by the PSO, are 0.735, 1.168, 0.610 and 1.015, 2.012, 3.060, respectively. As shown in Fig.1(c), the *DOF* of the optical needle is 6λ, and the full width at half maxima (*FWHM*) is 0.43λ, the electric field intensity of side-lobe is less than 15%, and the normalized electric field intensity is higher than 98%. The beam quality of the optical needle can be expressed as $\eta=\Phi_z/(\Phi_r+\Phi_z)$ and $\Phi_z=2\pi\int_0^{r_0}\left|E_z(r,0)\right|^2 r\mathrm{d}r$ (r_0 is the first zero point in the distribution of radial electric density). After calculation, the result of η is 96%. The result of η means that the optical needle with a strong longitudinally polarized composition in the focal space.

The generation of multi-segment optical needle is based on the generation of the single optical needle in the focal space. The optical needle with long focal depth and sub wavelength transverse resolution is generated a RPBG beam which modulated by the $T(\theta)$, and then the multi-segment optical needle sequences is further realized by coupling the multi-segment modulation function $P(z_d)$. Here, to obtain an optical needle with long *DOF*, sub wavelength transverse spot size and uniform intensity, it is necessary to balance the amplitude factor A_i and phase factor k_i. For the $T(\theta)$ in $M(\theta)$, the changes of amplitude factor A_i and phase factor k_i will cause distortion of the electric field distribution of the optical needle. Among them, if the phase factor is k_i too small or too large, the *DOF* of the optical needle will become longer or smaller, while if the amplitude factor A_i is too small or too large, the intensity uniformity of the optical needle will be directly affected. Therefore, the optimization of the algorithm is very important for the generation of optical needle. The setting of algorithm program and objective function can be seen from our previous research in Ref.[25].

After the single optical needle generated, the multi-segment optical needle sequence with different spacings and numbers can be generated by using the multi-segment modulation function $P(z_d)$. Based on the vector angular spectrum theory, Eqs.(2) and (3) are written as their angular spectrum forms, and Fourier transform is performed on them to obtain the Fourier transform form of their weighted fields, so that the phase distribution of the pupil plane behind the high *NA* objective can be calculated. The electric field distribution of the multi-segment optical needle sequence is determined by the convolution of the Fourier transform of the multi segment modulation function $P(z_d)$. According to the Fourier phase conversion theorem, the multi-segment modulation function $P(z_d)$ can realize the modulation of multi segment optical needle sequences with different numbers and distances on the optical axis. It is worth noting that the HF $M(\theta)$ is composed of the amplitude-phase transmission function $T(\theta)$ which generates the optical needle and the multi-segment modulation function $P(z_d)$. The generation of the multi-segment optical needle sequence is based on the generation of the single optical needle. The transmission function $T(\theta)$ and the multi-segment modulation function $P(z_d)$ that generate the optical needle can be considered to be mutually independent. Therefore, the multi-segment modulation function $P(z_d)$ is compatible. For the commonly used azimuthally polarized beams[13,14], by coupling the specially designed pure phase modulation filter $T(\theta)$ with the multi-segment modulation function $P(z_d)$, it is possible to generate the super resolution transverse polarization multi-segment optical needle sequences with long *DOF*, which is of great significance for the generation of multi-segment optical needle sequences by vector light fields with different polarization states.

To our best knowledge, for the multi-focal spots array which like multi-segment optical needle sequence, the multi-focal spots array with high spatial resolution not only requires the multi-focal spots array to have a clear profile distribution, but also ensures the focal spot in the multi-focal spots array with a high beam quality. Therefore, in the designing of the multi-segment optical needle sequence, the spacing and number of optical needles in

multi-segment optical needle sequence should be considered. On basis of the single optical needle, the multi-segment optical needle sequence with different spacing and numbers are further analyzed, respectively.

Fig.2(a)—(c) express the normalized electric field distribution of multi-segment optical needle sequences with different spacing. Each multi-segment optical needle sequence contains five optical needles, and the spacings of the optical needle in the multi-segment optical needle sequence are set as 8λ, 9λ, 10λ, respectively. The figure on the right is the phase diagram of the corresponding multi-segment optical needle sequence. As expected, the normalized intensity of the electric field distribution for the multi-segment needle sequence with different spacing (8λ, 9λ, 10λ) showed good uniformity, and there was almost no obvious interference between the optical needles in the multi-segment optical needle sequence, and each multi-segment optical needle sequence showed clear contour distribution. In addition, Fig.2(d)—(f) show the electric field distribution of multi-segment optical needle sequences with different number of optical needles, and the spacing of adjacent optical needles in each multi-segment light needle sequence is set as 8λ, and the number of the optical needles in the multi-segment optical needle sequences are 3, 4 and 6, respectively. For the multi-segment optical needle sequences with different numbers of optical needle, the distribution of the sequences' electric field still shows clear contour distribution, and the electric field distribution of the single optical needles in the sequences show a good homogeneity. It can be seen that the multi-segment optical needle sequence generated by HF can effectively ensure the electric field of the single optical needle, which makes HF more flexible and reliable in the designing and generation of the multi-segment optical needle sequence with different spacing or number.

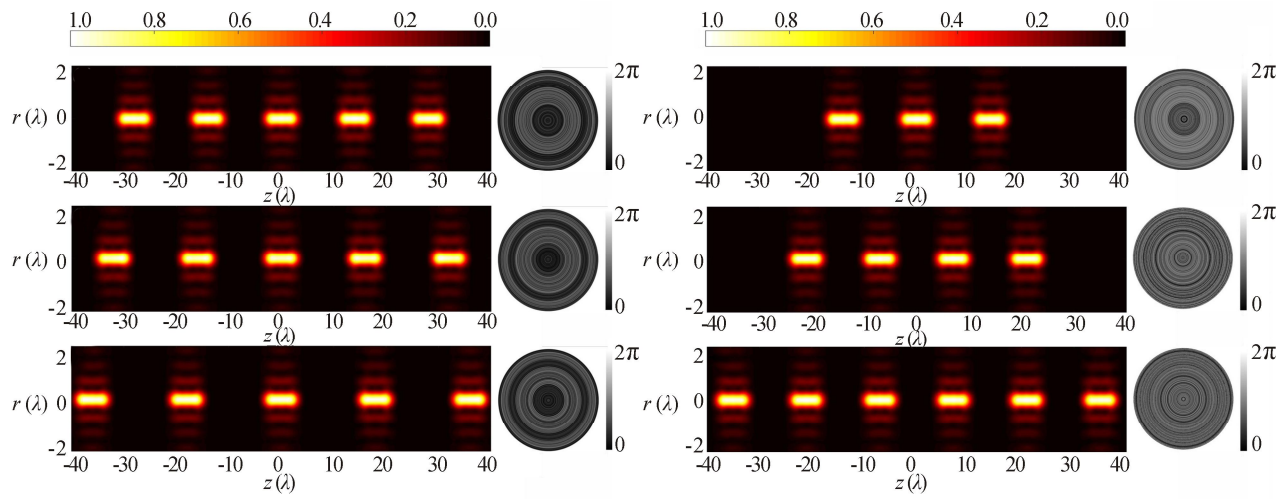

Fig.2 Normalized electric fields in the focal region of multi-segment optical needle sequence (Attached is the phase diagram of the light field): (a—c) Multi-segment optical needle sequences with different spacings (8λ, 9λ, 10λ); (d—f) Multi-segment optical needle sequences with different numbers of optical needles (3, 4, 6)

In order to quantitatively analyze the electric field distribution of the multi-segment optical needle sequences with different spacing and numbers of optical needles, we extracted the normalized electric field intensity curve of the multi-segment optical needle sequences, and the influence of the number and spacing of multi-segment optical needles on the single optical needle's electric field is further studied.

As we can see from Fig.3(a), the multi-segment optical needle sequences with different spacing (8λ, 9λ, 10λ), with the increase of the spacing, the uniformity of the electric field intensity for single optical needle is changed in different degrees. The normalized electric field intensity of the optical needle in each multi-segment optical needle sequence is above 90%. However, for the multi-segment optical needle sequences, with an adjacent optical needle spacing of 9λ, the uniformity of the sequence's electric field intensity is significantly lower than that of other optical needle sequences. It is worth noting that compared with the optical needle sequence with a spacing of 9λ, the intensity uniformity of electric field for the multi-segment optical needle sequence with a spacing of 10λ is significantly improved. According to our experience, the uniformity of electric field intensity for the optical needles in multi-segment optical needle sequence is mainly caused by the interference effect between adjacent optical needles. Therefore, reasonable setting the spacing of adjacent optical needles and effective optimization of the spatial structure of multi-segment optical needle sequence can make the multi-segment optical needle sequence have a good intensity homogeneity.

As a contrast, the intensity uniformity of the optical needles in the sequence is significantly less affected by

the number of optical needles. As shown in Fig.3(b), for the multi-segment optical needle sequences with three optical needles, the distribution of the electric field for the two outermost optical needles shows slight fluctuations, and the intensity uniformity of the single optical needle in the sequence is still higher than 90%. However, for the multi-stage optical needle sequence with four optical needles, the uniformity of the electric field intensity of the outermost two optical needles is further improved, and the uniformity of the electric field intensity for the optical needle is not significantly changed. Similarly, we still find similar changes in the light needle sequence with six light needles. By comparing the electric field distribution of multi-segment optical needle sequences with different distances and numbers, we can find that when the spacing of the optical needle changes, the interference effect of the multi-segment optical needle sequence is obviously changed. Thus, the uniformity of the electric field intensity for the internal single optical needle is changed. This shows that in the design and application of the multi-segment optical needle sequence, when the number of optical needles in the sequence is determined, the uniformity of the electric field intensity of the optical needles in the sequence can be improved by reasonably modulating the spacing of the optical needles, thus effectively improving the resolution of the multi-segment optical needle sequence in the focus spacing.

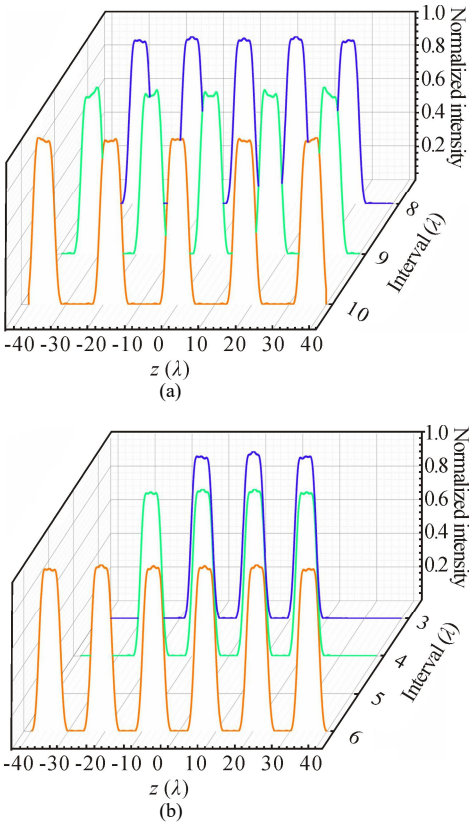

Fig.3 Curves of the normalized electric field intensity for the multi-segment optical needle sequences designed by HF: (a) Curves of normalized electric field intensity for the multi-segment optical needle sequences with different spacings (8*λ*, 9*λ*, 10*λ*); (b) Curves of normalized electric field intensity for the multi-segment optical needle sequences with different numbers of optical needles (3, 4, 6)

In conclusion, an HF coupled by a binary phase filter and a pure-phase filter is proposed to generate longitudinally polarized multi-segment optical needle sequences. Based on the vector diffraction theory, the binary phase filter optimized by the PSO algorithm is firstly used to the RPBG beam. In the high *NA* objective lens focusing system, a longitudinally polarized optical needle with sub-wavelength (0.430λ) transverse size and long *DOF* (6λ) is generated. The negligible sidelobe of optical needle is 15%, and the light field with high uniformity of 98% and high beam quality of 96%. Then modulated by the HF, the multi-segment optical needle sequence in the focal space can be garnered. The multi-segment optical needle sequences with different spacings and numbers of optical needles are generated in the focal volume. By analyzing the electric field distribution of multi-segment optical needle sequence, we found that the influence of the optical needle spacing on the intensity homogeneity of the multi segment optical needle sequence is much greater than that of the optical needles number in the multi-segment optical needle sequence. For the practical application, such as femtosecond laser processing, fluorescence imaging, optical trapping, the designing of the multi-segment optical needle sequence with a high spatial resolution can be realized by reasonably adjusting the spacing of the optical needles.

Ethics declarations

Conflicts of interest

The authors declare no conflict of interest.

References

[1] KOZAWA Y, SAKASHITA R, UESUGI Y, et al. Imaging with a longitudinal electric field in confocal laser scanning microscopy to enhance spatial resolution[J]. Optics express, 2020, 28(12)：18418-18430.

[2] WANG F M, XIAO Y, HUANG W, et al. Three-dimensional resolution enhancement in confocal microscopy with radially polarized illumination using subtractive imaging[J]. Optics communications, 2020, 458：124794.

[3] YANG Y, LUO M, LIU S, et al. Polarization-insensitive micro-metalens for high-resolution and miniaturized all-fiber two-photon microendoscopic fluorescence imaging[J]. Optics communications, 2019, 445：76-83.

[4] ZHANG Y, LIU X, LIN H, et al. Ultrafast multi-target control of tightly focused light fields[J]. Opto-electronic advances, 2022, 5(3)：210026-1-210026-12.

[5] SONG X. Three-dimensional optical bottle beams for

axial optical tweezers based on interference of Bessel beams[J]. Optical trapping and optical micromanipulation XVIII, International Society for Optics and Photonics, 2021：117982J.

[6] LI Y, HONG M. Parallel laser micro/nano-processing for functional device fabrication[J]. Laser & photonics reviews, 2020, 14(3)：1900062.

[7] MEIER M, ROMANO V, FEURER T, et al. Material processing with pulsed radially and azimuthally polarized laser radiation[J]. Applied physics A, 2007, 86：329-334.

[8] YU Y, HUANG H, ZHOU M, et al. Creation of a multi-segmented optical needle with prescribed length and spacing using the radiation pattern from a sectional-uniform line source[J]. Scientific reports, 2017, 7：10708.

[9] LAN T H, TIEN C H. Servo study of radially polarized beam in high numerical aperture optical data storage system[J]. Japanese journal of applied physics, 2007, 46：3758-3760.

[10] WANG H, SHI L, YUAN G, et al. Subwavelength and super-resolution nondiffraction beam[J]. Applied physics letters, 2006, 89：171102-171103.

[11] WANG H, SHI L, LUKYANCHUK B, et al. Creation of a needle of longitudinally polarized light in vacuum using binary optics[J]. Nature photonics, 2008, 2(8)：501-505.

[12] DIAO J, YUAN W, YU Y, et al. Controllable design of super-oscillatory planar lenses for sub-diffraction-limit optical needles[J]. Optics express, 2016, 24(3)：1924-1933.

[13] HAO X, KUANG C, WANG T, et al. Phase encoding for sharper focus of the azimuthally polarized beam[J]. Optics letters, 2010, 35(23)：3928-3930.

[14] WANG S, LI X, ZHOU J, et al. Ultralong pure longitudinal magnetization needle induced by annular vortex binary optics[J]. Optics letters, 2014, 39(17)：5022-5025.

[15] LI Y, RUI G, ZHOU S, et al. Enantioselective optical trapping of chiral nanoparticles using a transverse optical needle field with a transverse spin[J]. Optics express, 2020, 28(19)：27808-27822.

[16] HU H, GAN Q, ZHAN Q, et al. Generation of a nondiffracting superchiral optical needle for circular dichroism imaging of sparse subdiffraction objects[J]. Physical review letters, 2019, 122(22)：223901.

[17] GAO X Z, ZHAO P C, SUN X F, et al. Highly purified transversely polarized optical needle generated by the hybridly polarized vector optical field with hyperbolic symmetry[J]. Journal of optics, 2020, 22：105604.

[18] MAN Z, MIN C, DU L, et al. Sub-wavelength sized transversely polarized optical needle with exceptionally suppressed side-lobes[J]. Optics express, 2016, 24(2)：874-882.

[19] GAO X Z, ZHAO P C, ZHAO J H, et al. Sinusoidal-amplitude binary phase mask and its application in achieving an ultra-long optical needle[J]. Optics express, 2022, 30(15)：26275-26285.

[20] GOHN-KREUZ C, ROHRBACH A, et al. Light needles in scattering media using self-reconstructing beams and the STED principle[J]. Optica, 2017, 4(9)：1134-1142.

[21] YU Y, HUANG H, ZHOU M, et al. Creation of a multi-segmented optical needle with prescribed length and spacing using the radiation pattern from a sectional-uniform line source[J]. Scientific reports, 2017, 7：1-5.

[22] LUO J, ZHANG H, WANG S, et al. Three-dimensional magnetization needle arrays with controllable orientation[J]. Optics letters, 2019, 44(4)：727-730.

[23] RICHAEDS B, WOLF E. Electromagnetic diffraction in optical systems II. Structure of the image field in an aplanatic system[J]. Proceedings of the Royal Society of London. Series A, mathematical and physical sciences, 1959, 253：358-379.

[24] LEUTENEGGER M, RAO R, LEITGEB R A, et al. Fast focus field calculations[J]. Optics express, 2006, 14：11277-11291.

[25] SHI C, XU Z, NIE Z, et al. Sub-wavelength longitudinally polarized optical needle arrays generated with tightly focused radially polarized Gaussian beam[J]. Optics communications, 2022, 505：127506.